Characterization of Emissions and Residue from Measures to Improve Efficiency of *In Situ* Oil Burns

Brian K. Gullett[1], Johanna Aurell[2], Amara Holder[1], Nathan Lamie[3], Kemal Arsava[4], Robyn Conmy[5], Devi Sundaravadivelu[6], Karen Stone[7]

1. U.S. Environmental Protection Agency, Office of Research and Development, Center for Environmental Measurement and Modeling, Research Triangle Park, NC 27711, USA

2. University of Dayton Research Institute, 300 College Park, Dayton, OH 45469, USA

3. U.S. Army Corps of Engineers, Cold Regions Research Engineering Laboratory, 72 Lyme Road, Hanover, NH 03755, USA

4. Oak Ridge Institute for Science and Education Participant at U.S. Army Cold Regions Research Laboratory, 72 Lyme Road, Hanover, NH 03755, USA

5. U.S. Environmental Protection Agency, Office of Research and Development, Center for Environmental Solutions & Emergency Response, Cincinnati, OH 45219, USA

6. Pegasus Technical Services, Inc., 46 E. Hollister St, Cincinnati, OH 45219, USA

7. U.S. Department of the Interior, Bureau of Safety and Environmental Enforcement, Oil Spill Preparedness Division, 45600 Woodland Road, Sterling, VA 20166, USA

ABSTRACT NUMBER: 1141223

KEYWORDS: oil, burn, *in situ*, emissions, residues, spill

ABSTRACT

Simulated *in situ* oil burning tests were conducted in a 14 m x 2.4 m x 2.4 m tank to characterize variations in boom length/width aspect ratios, the use of injection air, nozzle angle,

and presence or absence of waves on combustion efficiency. Tests were done with approximately 35 L of unweathered Alaska North Slope oil within an outdoor, fresh water, 63 m^3 tank. The combustion plume was sampled with a crane-suspended instrument system. Emission measurements quantified carbon monoxide, carbon dioxide, particulate matter less than 2.5 μm ($PM_{2.5}$), and total carbon. Post-burn residue samples were collected with pre-weight oil absorbent to determining oil mass loss and total petroleum hydrocarbons (TPH) in the residue.

Plume measurements of modified combustion efficiencies (MCE_T) ranged from 85% to 93%. Measurement of residual, unburnt oil showed that the oil mass loss ranged from 89% to 99%. A three-fold variation in $PM_{2.5}$ emission factors was observed from the test conditions where the emission factors decreased with increased MCE. The TPH in the residue were found to decrease with increased oil mass loss percentage. In terms of combustion efficiency and oil consumption, results suggest that the most effective burns were those that have high length to width boom aspect ratios and added injection air.

INTRODUCTION

In-situ oil burns are often used to mitigate the potential environmental impact of floating oil originating from accidental/unintentional oil spills at sea. The resulting emissions have been characterized primarily for safety concerns related to worker inhalation exposure (Lane, 2011; Barnea, n.d.) and environmental pollution (Devai et al., 1998; Fingas, 2014). The black plumes resulting from combustion by-products have been characterized with respect to aerosol properties (Perring et al., 2011; Middlebrook et al., 2012), particulate matter equal to and less than 2.5 μm in mass median diameter ($PM_{2.5}$), and pollutants such as polycyclic aromatic hydrocarbons (PAHs), volatile organic compounds (VOCs) such as benzene, and trace amounts of polychlorinated dibenzodioxins and dibenzofurans (PCDDs/PCDFs) (Aurell and Gullett,

2010; Gullett et al., 2017). $PM_{2.5}$ is a criteria pollutant regulated by U.S. EPA as these small particles can be inhaled and cause adverse health effects to humans. Naphthalene, benzene, and PCDD/PCDFs can all be found on EPA's list of hazardous air pollutions (HAPs) (2008) as they have properties that are harmful to humans, marine life, and the environment.

Pollutants from *in situ* oil burns have been minimally quantified as emission factors (pollutant mass per mass of oil burned), with some exceptions (for example, (Ross et al., 1996)), limiting our ability to compare combustion efficiencies and technology improvements. Emission factors for $PM_{2.5}$ and VOCs from open burning sources have been found to decrease with increased modified combustion efficiencies (MCE) (Aurell et al., 2015; Aurell et al., 2017). For example, the $PM_{2.5}$ emission levels from burning of piles of timber slash were reduced five times when the MCE increased from 86.1% to 96.4% (Aurell et al., 2017).

This work aimed to characterize pollutants and unburned residues from *in situ* oil burns using variations in fire boom configurations, air-assist nozzle angles, and the presence or absence of waves.

METHODS

Test Set-up and Matrix

A wave tank of interior size 14 m × 2.4 m × 2.4 m (47 ft × 8 ft × 8 ft) located at U.S. Army Corps of Engineers, Cold Regions Research and Engineering Laboratory (CRREL) in Hanover, New Hampshire was used for the testing. The wave tank contained approximately 63 m^3 (16,700 gallons) of fresh water with a water level of 2.0 m (6.5 ft). The waves generated had a 12 cm amplitude and a 1.5 s period. A fire boom was positioned on the water surface and pre-weighed (approximately 31 kg (68 lbs) or 35 L (9.25 gallons)) Alaska North Slope crude oil was place inside the fire boom (Figure 1) to simulate *in situ* oil burning. The fire boom was equipped with

compressed air nozzles to optionally supply additional air to the *in situ* oil burn. The crude oil was ignited with a propane torch and the burns lasted for approximately 5 minutes. After a cooling period the residue was collected from the wave tank and weighed to derive the oil mass loss.

Three different boom configurations varied the length/width aspect ratios to 1:1, 4:1 and 9:1 (Figure 1). The enclosed area by the fire boom was kept constant at 3.4 m^2 resulting in the same crude oil thickness for each of the boom configurations. The air-assist nozzles were configured in three different angles; across the oil (90°), up over the oil (+45°), and down toward the oil (-45°). Emissions were measured from the different boom configurations when tested with or without waves, with or without air supply, as well as a combination of waves and supply of air resulting in fourteen different test setups. A total of sixteen burns were conducted with one of the setups replicated three times to establish the reproducibility of the tests. Due to the number of factors tested and limited resources such as funding and time, only one test setup was replicated.

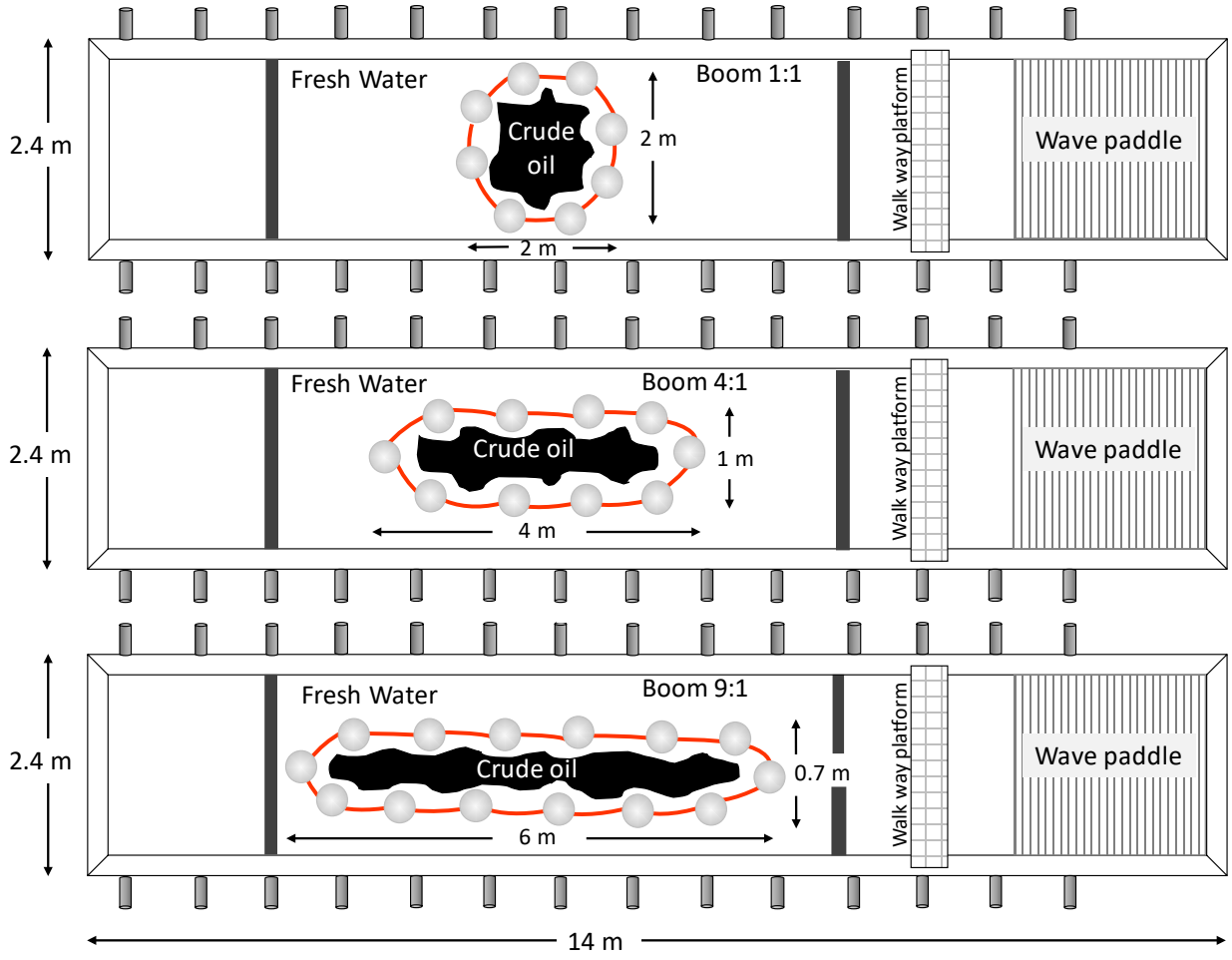

Figure 1. Schematic of CRREL's in-ground wave water tank with a 1:1, 4:1 and 9:1 aspect ratio fire boom. Boom dimensions approximate.

Measurements

The target pollutants, shown in Table 1, were sampled using an instrument system that was mounted on an aluminum skid which was suspended from a crane to easily maneuver the system into the burn plume. The carbon dioxide (CO_2) and carbon monoxide (CO) sensors were calibrated daily in accordance to EPA Method 3A (2017). $PM_{2.5}$ was collected using SKC's single-stage IMPACT Sampler (SKC Inc., USA) which collects $PM_{2.5}$ on a 47 mm teflon filter with a pore size of 2 µm via a Leland Legacy pump (SKC Inc., USA) with a constant flow rate

of 10 L/min. The PM filters were gravimetrically measured following procedures in 40 CFR Part 50, Appendix L (1987). The total carbon (TC), organic carbon (OC), and elemental carbon (EC) were collected on a 37 mm quartz filter using SKC's $PM_{2.5}$ single-stage Personal Modular Impactor (SKC Inc., USA) via a Gilian 5000 sampling pump (Sensidyne LP, USA) with a constant flow rate of 3 L/min. The TC/EC/OC filter samples were analyzed following NIOSH Method 5040 (1999) and Khan et al. (2012). The $PM_{2.5}$ and TC sampling pumps were calibrated with a Go-cal Air Flow Calibrator (Sensidyne LP, USA) prior to sampling.

Post-burn residue samples were collected with pre-weighed oil absorbent pads (New PIG Corp., Tipton, PA, USA) to determine oil mass loss and total petroleum hydrocarbons (TPH) using Gas Chromatography (GC) with Flame Ionization Detection (FID) using modified US EPA Method 8015D (n.d.). The TPH concentration was calculated using a six-point calibration curve generated with the unweathered oil used for the tests.

Table 1. Target pollutants.

Analyte	Method/Instruments	Frequency
CO_2	LiCOR-820, NDIR	Continuous
CO	Electrochemical cell	Continuous
$PM_{2.5}$	Impactor/filter/gravimetric	Batch
EC/OC/TC	Quartz filter	Batch
TPH	Adsorbent pads, GC-FID	Batch post-burn

Calculations

The oil mass loss was derived by subtracting the residue weight from the initial crude oil weight in each of the tests. The modified combustion efficiency (MCE_T) in this study includes TC from particles ($CO_2/(CO_2+CO+TC)$) and was calculated for each of the tests to establish how

well the oil burned in each of the different test conditions. The carbon mass balance approach was used to determine emission factors for each of the measured pollutants. The carbon mass balance assumes non-differential mixing of the plume pollutants. The sampled pollutant mass is divided by the co-sampled carbon mass (determined from CO and CO_2 measurements and particulate total carbon) and then multiplied by the carbon fraction of the fuel, 0.85 (Aurell and Gullett, 2010; Nelson, 1982). The derived emission factors are expressed as mass of pollutant per mass of initial oil. TPH in the residue is expressed as mass TPH per mass residue.

RESULTS AND DISCUSSION

Air Emissions

The results showed a linear (R^2 of 0.839) decrease of $PM_{2.5}$ emission levels with increased MCE_T values (Figure 2). Figure 2 also indicates that the 9:1 Boom Aspect Ratio (red markers) had lower $PM_{2.5}$ emission levels than the 1:1 Boom Aspect Ratio (yellow markers). By plotting the MCE_T and $PM_{2.5}$ emission levels as a function of Boom Aspect Ratio as shown in Figures 3a and 3b, it becomes apparent that the higher Boom Aspect Ratio results in higher MCE_T values and lower $PM_{2.5}$ emission levels regardless of adding additional injection air or in the presence of waves. The Boom Aspect Ratio effect is most probably due to air penetrating more efficiently into the thinner fuel rich zone of the 9:1 versus the 1:1 configuration (see Figure 1). The rate and extent of the combustion is limited by diffusion of oxygen into the region of volatilized fuel so the shorter penetration distance on the 9:1 configuration allows for more efficient combustion. The $PM_{2.5}$ emission factor for the replicate runs had a relative standard deviation (RSD) of 8% which indicates good reproducibility of the conducted tests. This RSD is lower than from a previous *in situ* oil burn study (25%) when a test scenario was replicated 14 times (Gullett et al., 2017).

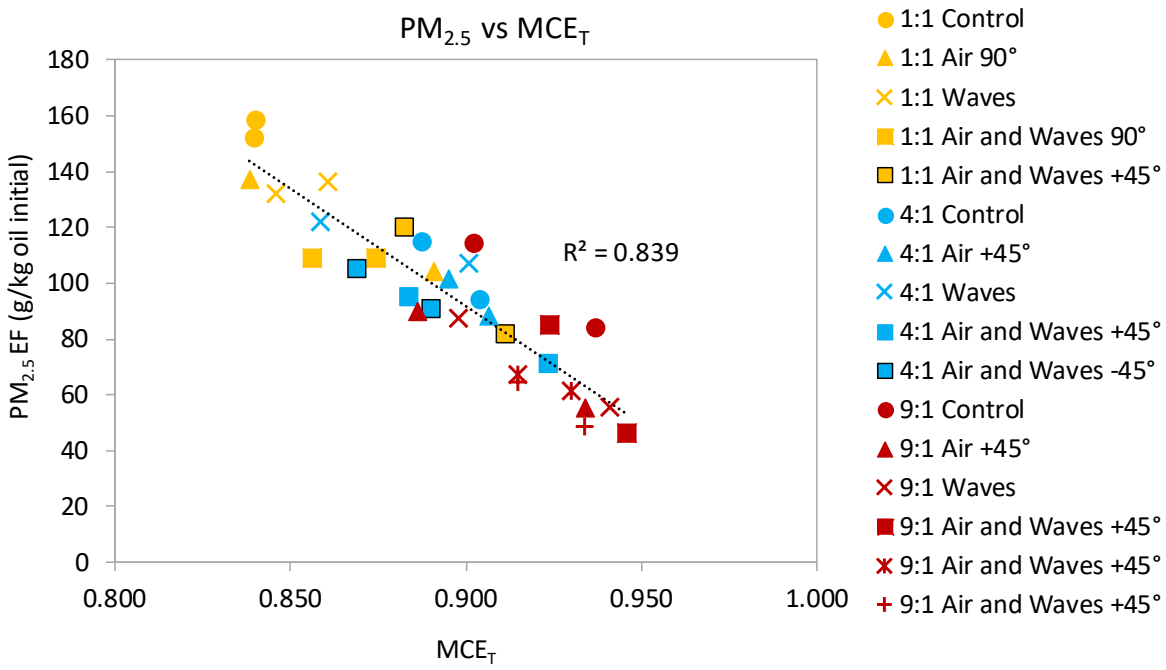

Figure 2. $PM_{2.5}$ emission factors versus modified combustion efficiency for each of the test runs (duplicate samples were collected per test run).

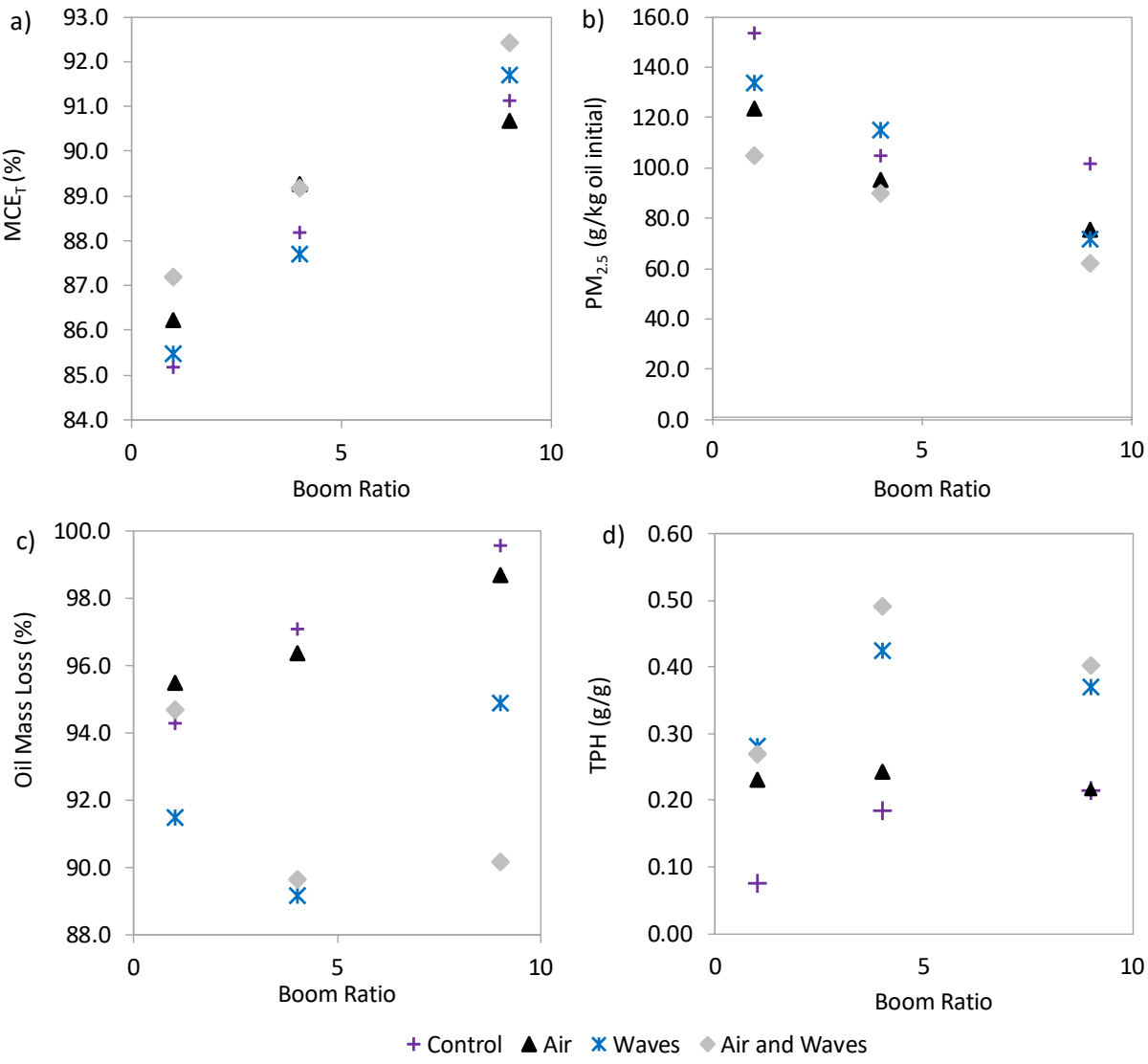

Figure 3. Boom Aspect Ratio versus a) modified combustion efficiency (MCE_T), b) $PM_{2.5}$ emission factors, c) oil mass loss percentage and d) total petroleum hydrocarbons (TPH) in the residue.

Residue

Oil mass loss varied from 88.8% to 99.6% (Table 2). A larger mass loss percentage was found with higher Boom Aspect Ratio but only when waves were absent (Figure 3c). The waves are speculated to circulate water which cools the bottom layer of the oil forcing the oil to reheat

for every passing wave. This reduces the heat transfer to the oil and the resulting oil vaporization, limiting combustion efficiency. The addition of injection air did not have any large effect on the mass loss as the Control tests had almost the same percentage as the Air tests. The three replicate runs had an RSD of 1.6% indicating very good reproducibility.

The TPH in the residue were found to decrease with increased percent oil mass lost (Figure 4a). No direct correlation could be found plotting the TPH as a function of Boom Aspect Ratio and MCE_T as shown in Figures 3d and 4b, respectively. This suggests that the oil vaporization (and TPH concentration) was not related to the subsequent air/fuel mixing and combustion efficiency. Although, a higher TPH concentration in the residue was found in tests when waves were added to Boom Aspect Ratios 4:1 and 9:1 indicating a decline in the percent of oil mass lost (Figures 3c and 3d). The TPH values are more related to the extent of burning (mass loss %) than the burn quality (MCE_T). When a greater fraction of original oil is burned (high mass loss), higher loss of organics occurred resulting in lower TPH concentration in the residue. For example, combustion quality may be very good (high MCE_T) but very little of the oil was burned (low mass loss). With low mass loss or extent of oil burned, a lower fraction of the oil will have been devolatilized and combusted, resulting in higher quantities of organics remaining in the residue (higher TPH concentration). A similar trend was observed in previous studies with lower mass loss resulting in higher TPH and PAH concentrations in the post-burn residue (Wang et al., 1999; Fingas, 2017). The increase of TPH in the residue when waves were added suggests that the waves negatively affect mass loss. The waves result in the oil slick oscillating lower into the water, resulting in greater heat loss to the water and less combustion efficiency. The TPH RSD for the replicate runs was 7% which indicates good reproducibility of the conducted test condition.

Table 2. Test matrix and oil mass loss percentage, modified combustion efficiency (MCE_T), $PM_{2.5}$ emission factors and mass total petroleum hydrocarbons (TPH) in the residue.

Burn Number	Test Condition	Configuration		Mass loss (%)	MCE_T (Unitless)	$PM_{2.5}$ (g/kg initial oil)	TPH (g/g residue)
		Boom Ratio	Nozzle location				
1	Control	1:1	No nozzle	94.3	0.840	154	0.075
2	Air	1:1	90°	95.5	0.860	124	0.231
3	Waves	1:1	No nozzle	91.5	0.851	134	0.280
4	Air and Waves	1:1	90°	94.4	0.861	109	0.262
5	Air and Waves	1:1	+45°	95.0	0.894	104	0.275
6	Control	9:1	No nozzle	99.6	0.917	102	0.213
7	Air	9:1	+45°	98.7	0.906	75	0.216
8	Waves	9:1	No nozzle	94.9	0.919	72	0.369
9	Air and Waves	9:1	+45°	89.2	0.935	66	0.371
10	Control	4:1	No nozzle	97.1	0.895	105	0.184
11	Air	4:1	+45°	96.4	0.900	95	0.242
12	Waves	4:1	No nozzle	89.2	0.878	115	0.424
13	Air and Waves	4:1	+45°	90.5	0.902	84	0.450
14	Air and Waves	4:1	-45°	88.8	0.879	98	0.529
15	Air and Waves	9:1	+45°	89.5	0.922	65	0.420
16	Air and Waves	9:1	+45°	91.8	0.924	57	0.416

Configuration: Boom Ratio = boom length/width, Nozzle orientation - degree of air nozzle to water/oil surface

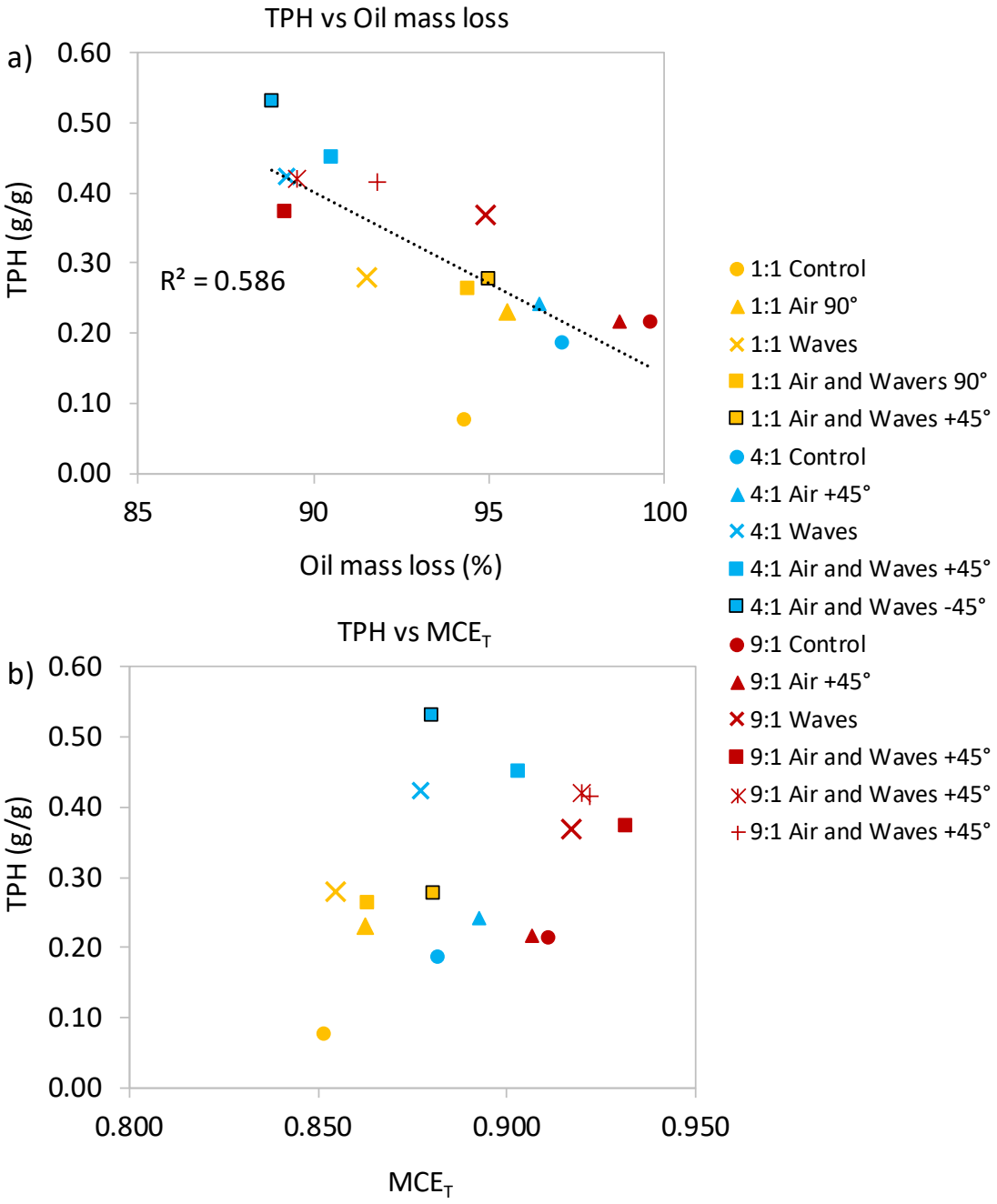

Figure 4. Total petroleum hydrocarbons (TPH) in the residue versus a) percent loss in post-burn residue b) modified combustion efficiency (MCE_T).

CONCLUSIONS

The $PM_{2.5}$ emission factor was found to decrease with increased combustion efficiency. The MCE_T and $PM_{2.5}$ emission factors ranged from 85% to 93% and 57 to 154 g/kg initial oil, respectively, corresponding to about three times lower $PM_{2.5}$ emission factor from the highest MCE_T to the lowest. Higher Boom Ratio configurations resulted in higher MCE_T regardless of added air or presence of waves.

Oil mass loss ranged from 88.8% to 99.6% where a higher oil mass loss occurred with higher Boom Aspect Ratios except when waves were present which always lowered the oil weight loss. The TPH in the residue was found to decrease with increased percent oil mass lost but no such correlation was found with MCE_T values. A higher TPH concentration was found when waves were added to the larger Boom Aspect Ratios.

ACKNOWLEDGEMENTS

This work was funded through an interagency agreement between the Department of Interior, Bureau of Safety and Environmental Enforcement and the U.S. EPA's Office of Research and Development. Messrs. Dale Greenwell, Bill Mitchell, and Dennis Tabor of U.S. EPA/ORD contributed critically to sampling, instrumentation, and analyses. Messrs. Brandon Booker and William Burch ably assisted with test execution and sampling.

DISCLAIMER

The views expressed in this article are those of the authors and do not necessarily represent the views or policies of the U.S. EPA. Mention of trade names or commercial products does not constitute endorsement or recommendation for use.

REFERENCES

40 CFR Part 50, Appendix L. 1987. Reference method for the determination of particulate matter as PM2.5 in the Atmosphere. https://www.gpo.gov/fdsys/pkg/CFR-2014-title40-vol2/pdf/CFR-2014-title40-vol2-part50-appL.pdf Accessed February, 2019

Aurell, J., and B. K. Gullett. 2010. Aerostat Sampling of PCDD/PCDF Emissions from the Gulf Oil Spill In Situ Burns. Environmental Science and Technology 44:9431-9437.

Aurell, J., B. K. Gullett, and D. Tabor. 2015. Emissions from southeastern U.S. Grasslands and pine savannas: Comparison of aerial and ground field measurements with laboratory burns. Atmospheric Environment 111:170-178.

Aurell, J., B. K. Gullett, D. Tabor, and N. Yonker. 2017. Emissions from prescribed burning of timber slash piles in Oregon. Atmospheric Environment 150:395-406.

Barnea, N. n.d. Health and Safety Aspects of In-situ Burning of Oil. National Oceanic and Atmospheric Administration. https://response.restoration.noaa.gov/sites/default/files/health-safety-ISB.pdf Accessed November 8, 2019

Devai, I., R. D. DeLaune, C. B. Henry Jr, C. W. Lindau, and P. O. Roberts. 1998. Environmental significance of atmospheric emission resulting from In situ burning of oiled salt marsh. Marine Environmental Research 45:157-167.

Fingas, M. 2014. Review of Emissions from Oil Fires. International Oil Spill Conference Proceedings 2014:1795-1805.

Fingas, M. 2017. The Fate of PAHs Resulting from In-Situ Oil Burns. International Oil Spill Conference Proceedings 2017:1041-1056.

Gullett, B. K., J. Aurell, A. Holder, W. Mitchell, D. Greenwell, M. Hays, R. Conmy, D. Tabor, W. Preston, I. George, J. P. Abrahamson, R. Vander Wal, and E. Holder. 2017. Characterization of emissions and residues from simulations of the Deepwater Horizon surface oil burns. Marine Pollution Bulletin 117:392-405.

Khan, B., M. D. Hays, C. Geron, and J. Jetter. 2012. Differences in the OC/EC Ratios that Characterize Ambient and Source Aerosols due to Thermal-Optical Analysis. Aerosol Science and Technology 46**:**127-137.

Lane, G. 2011. Air Quality Issues, Air Monitoring Needed for Cleanup Workers in Vessels. Deepwater Horizon Study Group -- Working Paper http://ccrm.berkeley.edu/pdfs_papers/DHSGWorkingPapersFeb16-2011/AirQualityIssuesAirMonitoringNeededForCleanupWorkersinVessels-GL_DHSG-Jan2011.pdf.

Middlebrook, A. M., D. M. Murphy, R. Ahmadov, E. L. Atlas, R. Bahreini, D. R. Blake, J. Brioude, J. A. de Gouw, F. C. Fehsenfeld, G. J. Frost, J. S. Holloway, D. A. Lack, J. M. Langridge, R. A. Lueb, S. A. McKeen, J. F. Meagher, S. Meinardi, J. A. Neuman, J. B. Nowak, D. D. Parrish, J. Peischl, A. E. Perring, I. B. Pollack, J. M. Roberts, T. B. Ryerson, J. P. Schwarz, J. R. Spackman, C. Warneke, and A. R. Ravishankara. 2012. Air quality implications of the Deepwater Horizon oil spill. Proceedings of the National Academy of Sciences of the United States of America 109:20280-20285.

Nelson, R. M., Jr. 1982. An Evaluation of the Carbon Balance Technique for Estimating Emission Factors and Fuel Consumption in Forest Fires. U.S. Department of Agriculture, Forest Service, Southeastern Forest Experiment Station, Asheville, NC, USA Research Paper SE-231.

NIOSH Method 5040. 1999. Elemental Carbon (Diesel Particulate). Issue 3, NIOSH Manual of Analytical Methods, 4th Ed., 30 September.

Perring, A. E., J. P. Schwarz, J. R. Spackman, R. Bahreini, J. A. de Gouw, R. S. Gao, J. S. Holloway, D. A. Lack, J. M. Langridge, J. Peischl, A. M. Middlebrook, T. B. Ryerson, C. Warneke, L. A. Watts, and D. W. Fahey. 2011. Characteristics of black carbon aerosol from a surface oil burn during the Deepwater Horizon oil spill. Geophysical Research Letters **38**:5.

Ross, J., R. Ferek, and P. Hobbs. 1996. Particle and Gas Emissions from an In Situ Burn of Crude Oil on the Ocean. Journal of Air Waste Management Association **46**:251-259.

Wang, Z., M. Fingas, Y. Y. Shu, L. Sigouin, M. Landriault, P. Lambert, R. Turpin, P. Campagna, and J. Mullin. 1999. Quantitative Characterization of PAHs in Burn Residue and Soot Samples and Differentiation of Pyrogenic PAHs from Petrogenic PAHs−The 1994 Mobile Burn Study. Environmental Science & Technology **33**:3100-3109.

U.S. EPA Hazardous Air Pollution List. 2008. Clean Air Act: Title 42 - The public health and welfare. U.S. Government Printing Office. http://www.gpo.gov/fdsys/pkg/USCODE-2008-title42/pdf/USCODE-2008-title42-chap85.pdf Accessed October 16 2019

U.S. EPA Method 3A. 2017. Determination of oxygen and carbon dioxide concentrations in emissions from stationary sources (instrumental analyzer procedure). https://www.epa.gov/sites/production/files/2017-08/documents/method_3a.pdf Accessed February 12, 2019

U.S. EPA Method 8015D. n.d. Nonhalogenated organics using GC/FID. https://www.epa.gov/sites/production/files/2015-12/documents/8015d_r4.pdf Accessed February 13, 2019